Measuring thermoelectric property of nano-heterostructure*

Lu Hong-Liang(路红亮), Zhang Chen-Dong(张晨栋), Cai Jin-Ming(蔡金明), Gao Min(高 敏), Zou Qiang(邹 强), Guo Hai-Ming(郭海明), and Gao Hong-Jun(高鸿钧)†

Beijing National Laboratory for Condensed Matter Physics and Institute of Physics, Chinese Academy of Sciences, Beijing 100190, *China*

(Received 6 May 2011; revised manuscript received 20 May 2011)

A method of measuring the thermoelectric power of nano-heterostructures based on four-probe scanning tunneling microscopy is presented. The process is composed of the *in-situ* fabrication of a tungsten–indium tip, the precise control of the tip-sample contact and the identification of thermoelectric potential. When the temperature of the substrate is elevated, while that of the tip is kept at room temperature, a thermoelectric potential occurs and can be detected by a current–voltage measurement. As an example of its application, the method is demonstrated to be effective to measure the thermoelectric power in several systems. A Seebeck coefficient of tens of μV/K is obtained in graphene epitaxially grown on Ru (0001) substrate and the thermoelectric potential polarity of this system is found to be the reverse of that of bare Ru (0001) substrate.

Keywords: thermoelectric property, four-probe scanning tunneling microscope, graphene, nano-heterostructure

PACS: 73.50.Lw, 81.05.ue, 68.37.Ef **DOI:** 10.1088/1674-1056/20/10/107301

1. Introduction

Nanoscale heterostructures have aroused much interest, owing to their promising applications in field-effect transistors, photodetectors, photodiodes, solar cells, catalysts[1,2] and refrigerators.[3] Many researchers have focused on the electron transport properties at their interfaces. When the temperatures on the two sides of an interface differ, thermoelectric voltage and current occur. Such nanosystems, if they each have a high thermoelectric figure of merit ZT ($ZT = S^2\sigma T/\kappa$, where S is Seebeck coefficient, σ the electrical conductivity, κ the thermal conductivity and T the absolute temperature), are very desirable for a wide range of applications such as nano-generators or energy harvesting,[4,5] nano-coolers,[5] and gas sensing.[6] How to measure the thermoelectric properties of nanostructures undoubtedly plays a key role in developing nanomaterials and nanostructures with high ZT. In the general method of measuring the Seebeck coefficient in nanosystems, a heater is located near the device to generate a temperature gradient, two resistors are utilized to monitor the temperature differences at two points on the nanodevices and then the thermoelectric voltage is measured by a voltmeter.[7,8] However, this method is not applicable for ultra thin nano-heterostructures because the temperature measurement is very difficult. The drawback of the existing method for thermoelectric property measurement has become a bottleneck in the development of nanomaterials with high ZT.

Graphene is a promising candidate for thermoelectric devices since a giant thermoelectric effect,[4] high thermal conductivity,[9] and a variety of other novel properties[10,11] have been demonstrated. However, most thermoelectric investigations have concentrated on the in-plane characteristics of graphene-based systems,[12] while little work has been done on heterostructures incorporating graphene. Recent successful preparations of epitaxially grown graphene on transition metal surfaces[13–17] have made it possible to study metal/graphene heterostructures, particularly their peculiar electronic structures and fantastic interfacial properties.

In this paper, we present our developed approach to using ultrahigh vacuum (UHV) 4-probe scanning tunneling microscopy (STM) to measure the thermoelectric properties in nano-heterostructures. The pro-

*Project supported by the National Natural Science Foundation of China (Grant No. 60976089) and the National Basic Research Program of China (Grant Nos. 2007CB936802 and 2009CB929103).

†Corresponding author. E-mail: hjgao@iphy.ac.cn

© 2011 Chinese Physical Society and IOP Publishing Ltd

cess is composed of the *in-situ* fabrication of tungsten–indium (W–In) tips, the precise control of the tip and the identification of thermoelectric potential. When there is a temperature difference between a substrate and a tip on it, a thermoelectric potential occurs and can be detected by the current–voltage (I–V) curves. Graphene on a transition metal system is taken as an example to verify the validity of this method. The agreement between experimental results and theoretical calculations indicates that this method is applicable for thermoelectric property characterization in nanostructures.

2. Experimental details

2.1. UHV four-probe STM system

Thermoelectric properties were measured using an Omicron UHV 4-probe STM system.[18,19] The base pressure was better than 2×10^{-8} Pa. An integrated scanning electron microscope (SEM) with a resolution of 20 nm was used to monitor the W–In tip preparation and to locate the features of interest on a sample. Each of the four probes could be positioned independently. The movement of each probe was controlled by a combination of a step motor and a piezo tube. The former allowed it to move three-dimensionally in a range of 10 mm×10 mm×5 mm; and the latter was responsible for the precise position in a range of 4 μm×4 μm×2.5 μm within an accuracy of 0.1 nm. Also, the sample stage could be moved in the X–Y plane, driven by a piezo creeper. The temperature of the sample stage could be varied within a range from 30 K to 500 K through liquid He or liquid N_2 cooling and an electrical heater.

In order to identify the thermoelectric potential, I–V curves were measured using a Keithley 4200-SCS Semiconductor Characterization System (Keithley 4200SCS). It is equipped with three independent source-measure units (SMUs) as well as their preamplifiers and capable of measuring a voltage down to 1 μV and a current lower than 1 fA. The Keithley 4200SCS is suited for the electrical measurement of nanostructures because it has a high input impedance, accurate current and voltage sources, and a high resolution.

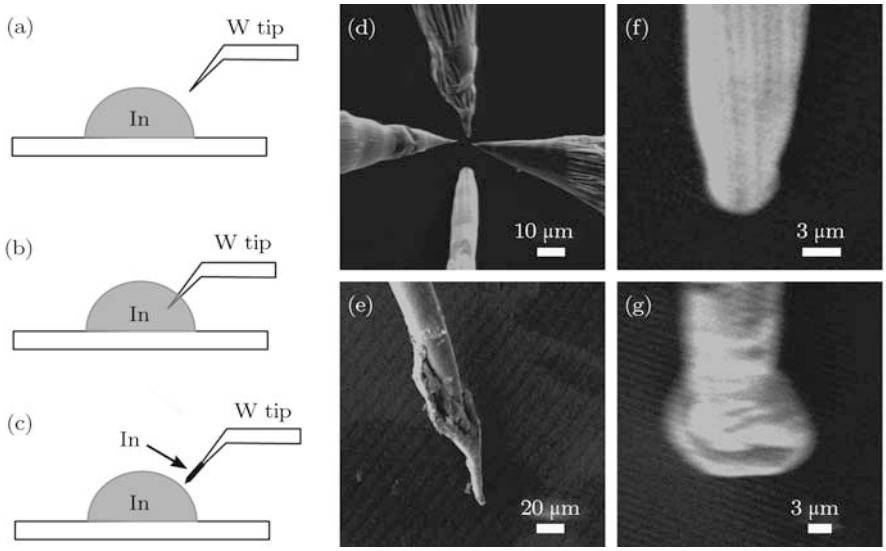


Fig. 1. Schematics showing the W–In tip preparation process ((a)–(c)) and SEM images of the W–In tips ((d)–(g)). (a) W tip ready for dipping, (b) W tip dipped in melted In droplet, (c) W tip withdrawn and coated with In, (d) four W–In tips ready for use, (e) the end of one W–In tip, coated with an In layer, (f) enlarged SEM image of a W–In tip, (g) a W–In tip in contact with a hot sample with deformation observable.

2.2. *In-situ* preparation of W–In tips

In order to make a soft tip-sample contact and prevent thin nanostructures from being damaged, it is necessary to prepare a special soft tip for measuring thermoelectric properties with a 4-probe STM. Indium is a desirable material for coating an STM tip because it is soft and electrically conductive with a low melting point. W tips were first prepared by a standard DC chemical etching method[20] immediately followed by transferring the tips to the UHV chamber to prevent oxidation. A drop of indium was melted in

the sample stage by electrical heating to 430 K. Then one W tip was dipped into the melted indium drop (Figs. 1(a) and 1(b)). A few seconds later, the W tip was drawn back and an indium layer formed at the end (Fig. 1(c)). Figures 1(d) and 1(e) show SEM images of as-prepared W–In tips. The surface of the W–In tip is clean due to its preparation in UHV, which is essential for the following measurement. Figures 1(f) and 1(g) display the W–In tips before and after contact with a hot sample surface. The deformation of W–In tips guarantees that the sample surface will not be damaged during measurement.

2.3. Preparation of monolayer graphene/Ru (0001) sample

A Ru (0001) crystal was cleaned in an UHV chamber using cycles of 0.6-keV Ar^+ sputtering followed by being annealed to a high temperature. A high quality monolayer graphene was fabricated by thermal decomposition of the hydrocarbon, ethylene on Ru (0001) metal substrate at high temperature. The amount of exposure was 100 Langmuir, sufficient for the formation of one layer of graphene. The detailed process is described elsewhere.[14,15,21] The perfect crystallinity of a graphene/Ru sample was confirmed by low energy electron diffraction (LEED) and STM before thermoelectric property measurement. Auger electron spectroscopy (AES) was used to analyse the chemical composition, and a sharp peak for carbon at 272 eV confirmed that carbon was present on the substrate.

2.4. Thermoelectric property measurement

Thermoelectric potential was obtained by measuring the I–V curves of the nanodevice system while the W–In tip and substrate were kept at different temperatures as shown in Fig. 2. After positioning the tip in the desired region with navigation of SEM, it can be brought onto the surface automatically by STM until the tunneling state is reached. Afterward we withdrew the tip by a step and switched the system to electrical measurement mode, at which time the voltage bias was applied to the tip with the Keithley 4200SCS. Then the tip was again brought onto the surface manually and slowly, and meanwhile the current was monitored. When a current was detected, we stopped approaching and began to measure I–V curves. A series of I–V curves was measured while the tip kept good contact with the sample.

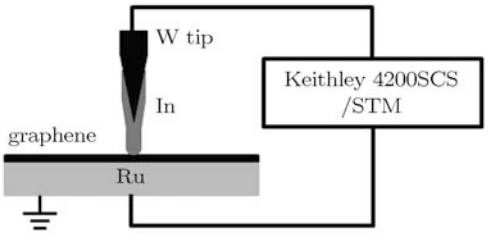


Fig. 2. Schematic diagram of the experimental setup for measuring I–V curves of graphene/Ru.

In addition, we can measure I–V curves using STM instead of the Keithley 4200SCS after engagement of the W–In tip. In the tunneling state, the feedback loop was turned off. Without withdrawing the tip, we applied a voltage to the tip and monitored the current through a preamplifier. We brought the tip onto the sample surface in steps of 1 Å∼10 Å (1 Å=0.1 nm) until a current was detected. Then I–V spectra were measured immediately. The thermoelectric potential can be derived from the I–V curves. One advantage of using STM to measure I–V curves is that there is no need to withdraw the tip, thereby making the measurement simplified. The limitation is that the smallest voltage step for I–V curve data acquisition is 0.25 mV, which is not sufficient to measure a small thermoelectric potential.

The temperature gradient was generated by heating the sample stage to a temperature preset by a Lakeshore 331 temperature controller. Because we measured the I–V curves immediately after the tip had contacted the sample surface, it was reasonable to believe that temperature difference was distributed mainly between the tip and the substrate. It was also observed that the offset voltage became smaller and smaller while the tip remained in contact, indicating that the temperature difference between tip and substrate became smaller. The Seebeck coefficient can be obtained by the equation $S = U/\Delta T$. Here, S, U, and ΔT are the Seebeck coefficient, thermoelectric potential, and temperature difference, respectively.

The lateral dimension of nanostructures to be measured is limited only by SEM resolution and tip radius. In our system, SEM resolution is better than 20 nm and W–In tip with tip radius less than 1 μm can be prepared, which indicates that thermoelectric properties of submicron devices could be measured in this method.

3. Results and discussion

Figure 3(a) shows a series of I–V curves from the Ru (0001) surface captured with the Keithley 4200SCS when the substrate temperature was increased to 450 K. Note that the slopes of these I–V curves are different, indicating that electrical resistance varies with the degree of contact between tip and substrate. However, all the curves show the same offset voltage when the current equals zero (they intersect the x axis at the same point), indicating a constant thermoelectric potential during each measurement. We define the thermoelectric potential pointing up as being positive in the setup of Fig. 2, i.e. the electron current (opposite to the electric current) driven by the temperature difference flows from the tip to the substrate. In this case, we can obtain a negative current at zero applied voltage, thus the current flows from the tip into Keithley 4200SCS. If we want to obtain zero current, we need to apply an opposite voltage equal to the thermoelectric potential. Therefore, the thermoelectric potential measured in the system is equal to the offset voltage on the x axis. From Fig. 3(a) a thermoelectric potential of -4 mV can be obtained for bare Ru (0001) substrate at 450 K.

We measured the thermoelectric potential of the samples from room temperature to high temperature (about 460 K). After each measurement for a group of I–V curves at a temperature, the W–In tip was withdrawn to prevent it from being heated up. When the sample temperature was increased to the next setpoint value, we approached the W–In tip again. Figure 3(b) shows the temperature-dependent thermoelectric potential of a W–In tip on monolayer graphene/Ru (0001), and for comparison, bare Ru (0001) substrate and highly oriented pyrolytic graphite (HOPG) were also investigated. The thermoelectric potential is negative on bare Ru (0001), and its magnitude increases linearly with temperature increasing. The Seebeck coefficient is about -27 μV/K, which is comparable to that of commercial thermocouples. The thermoelectric potential of HOPG is also negative but rather smaller, with a Seebeck coefficient of -5 μV/K. In the cases of Ru and HOPG substrates, when the substrate temperature is increased, electrons diffuse from hot substrate to cold W–In tips, so that a negative thermoelectric potential is generated. However, thermoelectric potential is positive in graphene/Ru (0001), and the corresponding Seebeck coefficient is 20 μV/K. The polarity of thermoelectric potential of graphene/Ru (0001) is reversed to that of Ru (0001), indicating a potential application of graphene materials as thermoelectric devices.

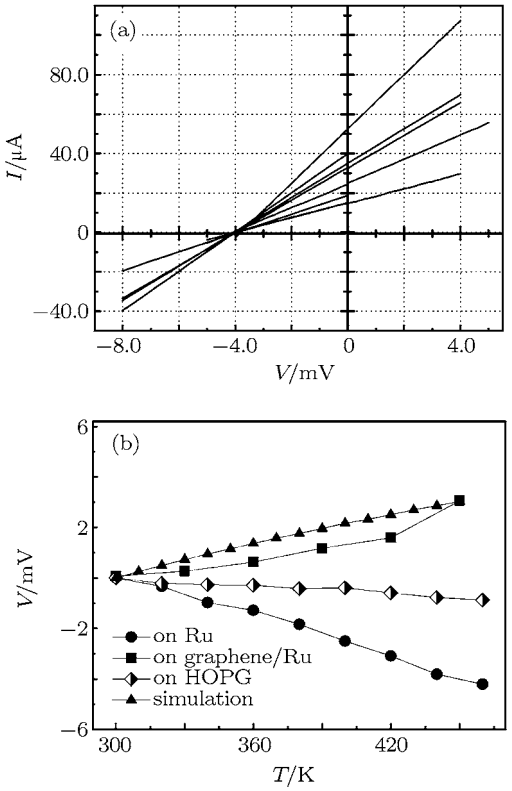


Fig. 3. (a) A series of I–V curves on bare Ru substrate obtained at 450 K with Keithley 4200SCS. All the curves intersect with the voltage axis at about -4.0 mV, indicating a stable thermoelectric potential; (b) experimentally obtained temperature-dependent thermoelectric potential of bare Ru (0001), monolayer graphene/Ru (0001), HOPG and the simulated result of graphene/Ru (0001).

The above results indicate that monolayer graphene plays a very important role in tuning the thermoelectric potential of this metal(tip)/graphene/metal(substrate) heterostructure. We investigated the atomic and the electronic structures of a graphene monolayer on Ru (0001) by using first-principles calculations and found that monolayer graphene can form periodical Moiré patterns with great corrugations on Ru (0001)[15,22] Specifically, the vertical difference between the highest and the lowest regions is more than 2 Å. Charge transfer between graphene and Ru leads to various carrier types in different regions of graphene, p-type in higher region and n-type in lower region. As is known, the electronic structure can influence the thermoelectric property greatly in semimetals[23] and semiconductors.[24] The thermoelectric potential polarity or electron flow direction depends on the carrier type, and different carrier types (n- or p-type) will generate reverse thermoelectric potential.[5] Leyo *et al.*[25] studied the local thermoelectric power of semiconductor nanoscale heterostructure and found that

in their system the carriers passing through the junction could be electrons and holes which determined the direction of thermoelectric power.

However, in our system, the carriers in two metal electrodes are always electrons. In order to explain how the carrier type in the central region determines the direction of thermoelectric power, we calculated the electron transmission coefficient and thermopotential in a model of metal/graphene/metal heterostructure by using the Landauer–Butticker formula. The model is composed of two metallic electrodes with a single layer of graphite (graphene) in between. The temperature of one electrode is fixed at room temperature (300 K), while the other is kept at a higher temperature. The transmission coefficient $T(E)$ and thermopotential were calculated with different carrier types of graphene and substrate temperatures (see our previous work for the calculation details[26]). It was found that in spite of metal electrodes, the carrier type of graphene determines the electron motion direction driven by the difference in temperature between the two electrodes. The electron current is along the thermal gradient direction for n-type graphene and against the thermal gradient direction for p-type graphene. Therefore for the graphene/Ru (0001) system, when the tip approaches the sample surface gently so that it only contacts the higher part (p-type) of graphene, a positive thermoelectric potential is obtained. The calculated thermoelectric potential of graphene/Ru is shown in Fig. 3(b), which is in good agreement with our experimental result.

Using this method, we also investigated the interfacial thermoelectric properties of monolayer graphene on Pt (111) and Ni (111) systems, which exhibited different graphene-substrate interactions and opposite carrier types of graphene. The results satisfactorily verified the predictions of our theoretical calculations[21,26] and confirmed the applicability of this method in measuring thermoelectric properties of nano-heterostructures.

4. Conclusions

We developed an experimental approach to measuring the Seebeck coefficient of nano-heterostructures by using a UHV four-probe STM system. With an *in-situ* elaborated tip in soft contact with the substrate at an elevated temperature, the thermoelectric potential is detected by measuring I–V curves. The application of this method to a monolayer graphene/Ru (0001) heterostructure shows a Seebeck coefficient of 20 μV/K and the thermoelectric potential polarity is found to be the reverse of that on bare Ru substrate. The results indicate that this method is helpful for investigating the thermoelectric properties of nano-heterostructures.

References

[1] Kundu P, Halder A, Viswanath B, Kundu D, Ramanath G and Ravishankar N 2010 *J. Am. Chem. Soc.* **132** 20

[2] Wu Y, Xiang J, Yang C, Lu W and Lieber C M 2004 *Nature* **430** 61

[3] He B X, He J Z and Miao G L 2011 *Acta Phys. Sin.* **60** 040509 (in Chinese)

[4] Dragoman D and Dragoman M 2007 *Appl. Phys. Lett.* **91** 203116

[5] Sales B C 2002 *Science* **295** 1248

[6] Adu C K W, Sumanasekera G U, Pradhan B K, Romero H E and Eklund P C 2001 *Chem. Phys. Lett.* **337** 31

[7] Boukai A I, Bunimovich Y, Tahir-Kheli J, Yu J K, Goddard W A and Heath J R 2008 *Nature* **451** 168

[8] von Arx M, Paul O and Baltes H 1997 *IEEE T. Semiconduct. M.* **10** 201

[9] Balandin A A, Ghosh S, Bao W Z, Calizo I, Teweldebrhan D, Miao F and Lau C N 2008 *Nano Lett.* **8** 902

[10] Novoselov K S, Geim A K, Morozov S V, Jiang D, Katsnelson M I, Grigorieva I V, Dubonos S V and Firsov A A 2005 *Nature* **438** 197

[11] Zhang Y B, Tan Y W, Stormer H L and Kim P 2005 *Nature* **438** 201

[12] Bao Z G, Chen Y P, Ouyang T, Yang K K and Zhong J X 2011 *Acta Phys. Sin.* **60** 028103 (in Chinese)

[13] de Parga A L V, Calleja F, Borca B, Passeggi M C G, Hinarejos J J, Guinea F and Miranda R 2008 *Phys. Rev. Lett.* **100** 056807

[14] Pan Y, Shi D X and Gao H J 2007 *Chin. Phys.* **16** 3151

[15] Pan Y, Zhang H G, Shi D X, Sun J T, Du S X, Liu F and Gao H J 2009 *Adv. Mater.* **21** 2777

[16] Coraux J, N'Diaye A T, Busse C and Michely T 2008 *Nano Lett.* **8** 565

[17] Pletikosic I, Kralj M, Pervan P, Brako R, Coraux J, N'Diaye A T, Busse C and Michely T 2009 *Phys. Rev. Lett.* **102** 056808

[18] Lin X, He X B, Lu J L, Gao L, Huan Q, Shi D X and Gao H J 2005 *Chin. Phys.* **14** 1536

[19] Lin X, He X B, Yang T Z, Guo W, Shi D X, Gao H J, Ma D D, Lee S T, Liu F and Xie X C 2006 *Appl. Phys. Lett.* **89** 043103

[20] Muller A D, Muller F, Hietschold M, Demming F, Jersch J and Dickmann K 1999 *Rev. Sci. Instrum.* **70** 3970

[21] Gao M, Pan Y, Zhang C D, Hu H, Yang R, Lu H L, Cai J M, Du S X, Liu F and Gao H J 2010 *Appl. Phys. Lett.* **96** 053109

[22] Sun J T, Du S X, Xiao W D, Hu H, Zhang Y Y, Li G and Gao H J 2009 *Chin. Phys.* B **18** 3008

[23] Pan Z J, Zhang L T and Wu J S 2005 *Acta Phys. Sin.* **54** 328 (in Chinese)

[24] Pan Z J, Zhang L T and Wu J S 2005 *Acta Phys. Sin.* **54** 5308 (in Chinese)

[25] Lyeo H K, Khajetoorians A A, Shi L, Pipe K P, Ram R J, Shakouri A and Shih C K 2004 *Science* **303** 816

[26] Hu H, Cai J M, Zhang C D, Gao M, Pan Y, Du S X, Sun Q F, Niu Q, Xie X C and Gao H J 2010 *Chin. Phys.* B **19** 037202